Journal of the Meteorological Society of Japan

EARLY ONLINE RELEASE

The DOI for this manuscript is
DOI:10.2151/jmsj.2022-045
J-STAGE Advance published date: July 22nd, 2022
The final manuscript after publication will replace the preliminary version at the above DOI once it is available.

Heavy Snowfall at Iwamizawa Influenced by the Tsushima Warm Current

Kazutoshi SATO[1], Takao KAMEDA, and Tatsuo SHIRAKAWA

Kitami Institute of Technology, Kitami 090-8507, Japan

Submitted to *Journal of the Meteorological Society of Japan*

September 3, 2021

Revised to *Journal of the Meteorological Society of Japan*

July 1, 2022

----

1) Corresponding author: Kazutoshi Sato, Kitami Institute of Technology, 165 Koen-cho, Kitami 090-8507, Hokkaido, Japan

Email: satokazu@mail.kitami-it.ac.jp

Tel: +81-1-5726-9429

Abstract

Iwamizawa on the Sea of Japan side of Hokkaido is one of the cities in Japan that experience frequent heavy snowfall events. Warm surface-layer ocean anomalies over the Sea of Japan can induce heavy snowfall over the Sea of Japan side of Japan; however, the relationship between ocean temperature over the northern Sea of Japan and snowfall events at Iwamizawa remains uncertain. This study used reanalysis data to investigate atmospheric and oceanic circulation anomalies associated with each anomalous heavy snowfall winter month at Iwamizawa. During all anomalous snowfall winter months at Iwamizawa, a cold air anomaly with northwesterly winds existed over the Far East that was associated with a dipole pattern with anticyclone anomalies over the north coast of the Eurasian Continent and cyclonic anomalies extending zonally over the Far East and northern Pacific Ocean. The surface cold air temperature and strong wind speed anomalies are major factor for anomalous upward turbulent heat flux over the northern Sea of Japan during all anomalous snowfall winter months at Iwamizawa. Additionally, during anomalous snowfall January, warm surface-layer ocean anomaly over the northern Sea of Japan, which preceded the heavy snowfall events at Iwamizawa by two months, has an important role in upward turbulent heat flux anomaly. This preceding warm ocean temperature anomaly was associated with a strong Tsushima Warm Current anomaly. Results showed that warm surface-layer ocean anomaly over the northern Sea of Japan that precedes anomalous cold advection from the Eurasian Continent has also large impact on producing heavy snowfall events over western Hokkaido coastal regions near Iwamizawa in January.

Keywords: Tsushima Warm Current; Sea of Japan; heavy snowfall; Iwamizawa

1. Introduction

During the winter monsoon season, the Siberian High over Eurasia and a developed cyclone over the North Pacific create a strong surface pressure gradient over East Asia. The northwesterly winter monsoon associated with this strong pressure gradient leads to outbreaks of cold air from the Eurasian Continent toward Japan. The relatively warm ocean provides a rich supply of water vapor and heat to the cold and dry air moving over the Sea of Japan, resulting in development of convective clouds that can cause extreme weather with heavy snowfall (e.g., Ninomiya 1968; Yoshizaki et al. 2004; Inoue et al. 2005; Sato et al. 2017).

Takano et al. (2008) reported that air mass modification over the Sea of Japan is strongly related to a large-scale atmospheric north–south dipole pattern (similar to the western Pacific (WP) pattern). When the phase of the WP pattern is negative (positive), the winter monsoon is enhanced (reduced) over East Asia, causing anomalous cold (warm) winters over the Far East (Takaya and Nakamura 2013). Additionally, cold air over the Eurasian Continent moves eastward with the movement of a trough in the middle troposphere (Hori et al. 2011). Several mechanisms regarding anomalous cold temperature over the Eurasian Continent have been reported in previous studies (Honda et al. 2009; Inoue et al. 2012; Sato et al., 2014, Nakanowatari et al. 2014, Mori et al. 2014, Nakamura et al. 2015). The decline of sea ice over the Barents and Kara seas strengthens the Siberian High through enhanced release of oceanic heat (Honda et al. 2009; Nakanowatari et al. 2014, Mori et al. 2014), and a poleward shift of cyclone tracks (Inoue et al. 2012) leads to anomalous cold temperatures over the Eurasian

Continent. The atmospheric response to changes in the Atlantic warm ocean current (i.e., the Gulf Stream) has direct and indirect effects on cold temperature anomalies over Eurasia (Sato et al. 2014).

Anomalous warm sea surface temperature (SST) around Japan has direct impact on the weather over Japan (Manda et al. 2014, Ando et al. 2015). Therefore, the relationships between SST over the Sea of Japan and precipitation over the Sea of Japan side of Japan have been investigated in previous studies (Sato and Sugimoto 2013, Takahashi et al. 2013, Takahashi and Idenaga 2013, Yasunaga and Tomochika 2017). During autumn and winter, positive SST trends are observed over the northern Sea of Japan from the 1980s to the 2000s or 2010s (Sato and Sugimoto 2013, Yasunaga and Tomochika 2017). Numerical experiments have revealed that anomalous upward latent heat flux associated with the warm SST anomaly over the Sea of Japan enhances snowfall over Sea of Japan side regions of Japan (Takahashi et al. 2013). During winter, the amount of precipitation over Sea of Japan side regions can increase on the timescale of a few days following an increase in SST over the Sea of Japan (Takahashi and Idenaga 2013). In contrast, in the same winter month, there is no relationship between monthly mean precipitation over the Sea of Japan side and SST over the Sea of Japan (Yasunaga and Tomochika 2017). This is because there are month-to-month variances of SST over the Sea of Japan in winter months during a strong winter monsoon (Takano et al. 2008). Therefore, the amounts of monthly precipitation over Sea of Japan side regions in December are correlated significantly with the 1-month prior SST over the Sea of Japan (Takano et al. 2008, Yasunaga and Tomochika 2017). Warm ocean currents have important roles in changing local and large-scale precipitation systems (Hirose and Fukudome 2006; Kunoki et al. 2015, Sato et al. 2014, 2015, 2021; Minobe et al. 2008, 2010; Minobe and Takebayashi 2015). Specifically, in the Sea of Japan, the stronger transport of the Tsushima Warm Current (TWC) during autumn causes a warm SST anomaly over the southern Sea of Japan, enhancing winter snowfall over the Sea of Japan side of Japan (Hirose and Fukudome 2006; Hirose et al. 2009; Sugimoto and Hirose 2014).

Numerous studies have investigated snowfall amounts over Hokkaido, which is one of the regions of Japan that experience heavy snowfall during the winter monsoon season (Campbell et al. 2018; Shirakawa and Kameda 2019; Inatsu et al. 2020; Kawazoe et al. 2020; Takahashi 2021). When the northwesterly winter monsoon is intensified over the Sea of Japan, the cloud band associated with heavy snowfall events can be observed to extend from the northern Sea of Japan to western Hokkaido (Muramatsu 1979; Fujiyoshi et al. 1992, 1998; Katsumata et al. 1998, 2000; Yoshimoto et al. 2000). A part of cloud band initially forms on the lee side of Russia's Sikhote-Alin mountain range on the east coast of the Eurasian Continent owing to topographic effects of the mountains (Muramatsu 1979; Ohtake et al. 2008). Additionally, convective clouds associated with mesoscale systems (i.e., polar lows) bring heavy snowfall over western parts of Hokkaido (Ninomiya 1994). When the Sea of Okhotsk is covered with sea ice, cold advection from the sea ice area influences on formations and intensifications of these mesocale systems (Tsuboki et al. 1989).

The continual cloud band is formed over the Sea of Japan during the winter months, leading to relatively large climatological total amounts of snowfall in western parts of Hokkaido compared with eastern parts of Hokkaido (Fig. 1). Specifically, anomalous heavy snowfall at Iwamizawa in western Hokkaido is often greater in comparison with that at other stations in Hokkaido. During the 2020/2021 winter season, Iwamizawa experienced four extreme heavy snowfall events (Fig. 2a). Although a strong snowfall band associated with a mesoscale system was observed during the snowfall event near the end of February 2021 (Fig. 2e), snow cloud bands formed over western coastal regions of Hokkaido during the other three snowfall events that occurred in December 2020 and early February 2021 (Fig. 2b–d). There has been no study previously on the relationship between the surface-layer ocean temperature anomaly over the northern Sea of Japan and anomalous snowfall at Iwamizawa. This study investigated the atmospheric and oceanic circulation anomalies associated with anomalous winter snowfall at Iwamizawa.

2. Data and Method

To investigate the atmospheric and oceanic fields, monthly mean Climate Forecast System Reanalysis data from January 1979 to March 2011 and Climate Forecast System Version 2 data after April 2011 were used in this study. The National Centers for Environmental Prediction produces both these datasets on 0.5° × 0.5° grids (Saha et al. 2010, 2014). The data include meteorological (e.g., temperature, wind, specific humidity, geopotential height, turbulent heat flux and radiative heat flux) and oceanographic (e.g., potential ocean temperature and ocean current) parameters at various levels. The atmospheric fields during winter 2020/2021 were based on Japan Meteorological Agency (JMA) Meso Scale Model data (MSM), which are provided after July 2002 (Fig. 2b–d). We supplemented in situ data with gridded analyses of precipitation derived from radar data after June 2003 provided by the JMA. Additionally, we used monthly total snowfall (MTS) data from 116 stations of the Automated Meteorological Data Acquisition System (AMeDAS) in Hokkaido (Fig. 1).

To understand interannual snowfall variations at Iwamizawa, we focused on time series of MTS anomalies during each winter month (i.e., December, January, and February) at Iwamizawa (Fig. 3). Referring to this time series, we selected typical heavy and light snowfall years for which snowfall values exceed 0.7 standard deviations for each winter month. To compare the broad atmospheric and oceanic circulations, we compiled difference maps of atmospheric and oceanic fields by subtracting composites for heavy versus light snowfall winter months. Moreover, we calculated correlation coefficients for MTS at Iwamizawa with atmospheric and oceanic parameters for all winter months.

To assess the contributions from SST anomaly (SSTA), surface air temperature anomaly (SATA) and surface wind speed anomaly (SWSA) to sensible and latent heat flux anomalies, we used the equations reported by Tanimoto et al. (2003). The sensible and latent heat fluxes are given as the sum of climatological mean and anomaly. Therefore, the anomalous sensible and latent heat fluxes are expressed below:

$$Q_E' = Q_E - \overline{Q_E} = \rho_a L C_E\{\overline{U} q_s' - \overline{U} q_a' + U'(\overline{q_s} - \overline{q_a}) + [U'(q_s' - q_a') - \overline{U'(q_s' - q_a')}]\} \quad (1)$$

$$Q_H' = Q_H - \overline{Q_H} = \rho_a c_p C_H\{\overline{U} T_s' - \overline{U} T_a' + U'(\overline{T_s} - \overline{T_a}) + [U'(T_s' - T_a') - \overline{U'(T_s' - T_a')}]\} \quad (2)$$

Q_E and Q_H are the latent and sensible heat fluxes, respectively. Here, ρ_a is the air density with the value of 1.293 kg m^{-3}, L the latent heat of vaporization for water with the value of 2.50×10^6 J kg^{-1}, c_p the specific heat of air at constant pressure with the value of 1004 J kg^{-1} K^{-1}, U is the wind speed, and C_E and C_H are transfer coefficients for Q_E and Q_H, respectively. Subscripts s and a indicate values at the sea surface and 2 m height, respectively. Overbars and primes indicate the climatological mean and the deviation from it. The first three terms of equations (1) and (2) are considered to represent the respective contributions from SSTA, SATA and SWSA to sensible and latent heat fluxes (Tanimoto et al. 2003).

In addition, we estimated the contributions from horizontal ocean temperature advection ($-OV \cdot \nabla OT - OU \cdot \nabla OT$) to heat balance in the surface-layer ocean. Here, OT denotes the surface-layer ocean temperature, OV and OU denote the surface-layer meridional and zonal ocean current, respectively.

3. Results

3.1 Atmospheric circulations causing heavy snowfall winters in northern Japan

Figure 4a–c shows difference maps of temperature at 950 hPa (T950) with sea level pressure between heavy and light snowfall years at Iwamizawa for each winter month. In heavy snowfall years of all winter months, the T950s have significant cold temperature anomalies over the Far East. Dipole patterns with an anticyclonic anomaly over the Eurasian Continent and a cyclonic anomaly over the northern Pacific Ocean can be seen during all heavy snowfall winter months. These patterns cause a pressure gradient over the Far East that induces northwesterly cold advection anomalies over northern Japan. The frequency of formation of cloud bands with heavy snowfall, extending from the eastern Eurasian Continent to western Hokkaido, would be increased by northwesterly cold advection anomalies. In the upper troposphere, the differences in geopotential height at 300 hPa (Z300) has a dipole pattern with anticyclone anomalies over the north coast of the Eurasian Continent and cyclonic anomalies extending zonally over the Far East and northern Pacific Ocean (Fig. 4d–f). In heavy snowfall winters, the WP pattern, which enhances northerly cold advection associated with the winter monsoon, increases the amount of snowfall over Hokkaido (Inatsu et al. 2021). However, there is no correlation coefficient between the MTS and WP index (available from https://psl.noaa.gov/data/climateindices/list) for all months during 1979 and 2020/2021 (December, January: $|r|=0.0$; February: $|r|=0.2$), indicating that this dipole pattern is different from the WP pattern.

The propagation of wave-activity flux, which represents propagation of quasi-stationary Rossby waves, indicates that a wave train appears from the northern Eurasian Continent to the Far East (Fig. 4d–f). Although anomalous sea ice decline over the Barents–Kara seas is known to induce an anticyclonic anomaly over the Barents–Kara sector (Honda et al. 2009, Inoue et al. 2012, Mori et al. 2014, Sato et al. 2014), statistically significant decline in sea ice in the Barents–Kara seas is not evident during heavy snowfall years for all winter months (Fig. 4d–f). The covered sea ice reduces heat releasing from ocean and causes no significant differences in upward turbulent heat fluxes over the Barents–Kara sector in all heavy snowfall months (not shown). Additionally, during all winter months in heavy snowfall years, there are also no differences in other factors that might influence this atmospheric circulation anomaly (e.g., a weakened polar vortex in the stratosphere, as reported by Nakamura et al. (2015) and poleward movement of the Gulf Stream, as reported by Sato et al. (2014)). Teleconnections between the tropical regions and the Arctic are not seen in all heavy snowfall months, suggesting that change in another factor over the high latitudes could influence these atmospheric circulation anomalies. In contrast, during heavy snowfall February months, there is statistically significant positive anomaly in sea ice concentration over the Sea of Okhotsk (Fig. 4f). The relatively cold air mass associated with heavy sea ice cover would influence on formation of convergent cloud with heavy snowfall reported by previous study (Tsuboki et al. 1989). In fact, during 23 and 24 February 2021, the heavy snowfall event was induced by mesoscale systems (Fig. 2a,e).

To further investigate the relationship between MTS and atmospheric circulation for each winter month, we calculated the correlations between MTS at Iwamizawa and atmospheric parameters (T950 and Z300) for the three winter months (Fig. 5). Air temperature in the lower troposphere (T950) over the Far East has significant negative correlation with MTS at Iwamizawa in all winter months, with particularly strong negative correlation ($|r|>0.6$) over northern Japan (Fig. 5a–c). In the upper troposphere, there are statistical relationships between MTS at Iwamizawa and the dipole pattern, with negative correlation (|r|>0.5) over the northern Pacific Ocean and positive correlation (|r|>0.3) over the northern Eurasian Continent in all winter months (Fig. 5d–f). The high correlations between MTS at Iwamizawa and atmospheric variations, which indicate that anomalous cold advection associated with the meridinal dipole pattern has an important role in Iwamizawa snowfall, are in agreement with the findings of previous studies (Hirose and Fukudome 2006, Takano et al. 2008, Takahashi and Idenaga 2013).

3.2 Tsushima Warm Current causing a warm surface-layer ocean anomaly over the northern Sea of Japan

To investigate surface-layer ocean temperature anomalies in heavy snowfall years, we examined difference maps of ocean temperature in the surface layer (5-m depth) between heavy and light snowfall years at Iwamizawa for all winter months (Fig. 6). In heavy snowfall December months, although there are positive differences in surface-layer ocean temperature over the northern Sea of Japan, the amplitude of this warm anomaly is small (Fig. 6a). In contrast, difference maps of surface-layer ocean temperature during the months prior (October and November) to heavy snowfall December months (Fig. 6b and c) reveal a statistically significant warm anomaly around Ishikari Bay. The correlation coefficient between MTS at Iwamizawa during December and surface-layer ocean temperature during prior months (November and October) shows that although the correlations have relatively small magnitude over the northern Sea of Japan, there are significant positive correlations over Ishikari Bay (Fig. 7b, c).

The difference in ocean current velocity in the surface-layer shows eastward and northeastward ocean current anomalies from the Sea of Japan to Ishikari Bay (Fig. 6b and c), suggesting that a strong TWC anomaly would have an impact on the warm surface-layer ocean anomaly over Ishikari Bay. To estimate the impact of ocean current anomaly associated with the strong TWC anomaly on the surface-layer ocean temperature anomaly, we made difference maps of contribution from horizontal ocean temperature advection to change in surface-layer ocean temperature between heavy and light snowfall years at Iwamizawa for all winter months (Fig.8). Although the increase in horizontal advection associated with the strong TWC anomaly during October would contribute to the warm surface-layer ocean anomaly over Ishikari Bay during November (Figs. 6b and 8c), there is the small magnitude of horizontal ocean temperature advection anomaly with no statistically significant during October (Fig. 8c). To assess the impacts of atmospheric variations on the warm surface-layer ocean anomaly, we calculated surface heat flux, which consists of turbulent and radiative heat fluxes. Figure 9 shows difference maps of surface heat flux between heavy and light snowfall years at Iwamizawa for all winter months. During the months prior to heavy snowfall December months, there are no positive differences in surface heat flux over the northern Sea of Japan (Fig. 9b and c). These analyses suggest that other oceanic parameters (e.g. diffusion and the entrainment through the bottom boundary of the mixed layer) would be a major factor for the warm surface-layer ocean anomaly during the months prior to heavy snowfall December months. However, the data assimilation would influence the surface-layer temperature anomaly.

In heavy snowfall January months, the ocean temperature in the surface layer has a warm anomaly in coastal regions of the Siberian continent (Fig. 6d). During the prior months (December and November) of heavy snowfall January months, the magnitude and distribution of statistically significant warm surface-layer ocean anomalies are larger than those in the prior months (November and October) of heavy snowfall December months (Fig. 6b, c, e, and f), suggesting that the warm ocean temperature anomalies remain even during heavy snowfall January months (Fig. 6d). The positive correlations between surface-layer ocean temperatures during prior months and MTS during January months are seen over the Siberia coastal regions (Fig. 7e and f). These positive correlation patterns are similar to those of warm surface-layer ocean anomalies in the prior months of heavy snowfall January months (Figs. 6e, and f and 7e, and f). The preceding warm surface-layer ocean temperature anomaly over the Sea of Japan would influence MTS at Iwamizawa in January. During two prior months of heavy snowfall January months, over the Siberia coastal regions, northward ocean current anomalies, which are associated with a strong northward TWC, are seen over these preceding warm surface-layer ocean anomalies (Fig. 6e and f). There are positive differences in horizontal ocean temperature advection over the Siberia coastal regions (Fig. 8e and f), indicating that the warm horizontal advection anomaly associated with the strong TWC anomaly is large enough to cause the warm surface-layer ocean anomaly during two prior months of heavy snowfall January months. In contrast, the significant positive differences in surface heat flux are not observed over significant warm surface-layer ocean anomaly areas (Fig. 9e and f). Therefore, atmospheric parameters have small impact on these warm surface-layer ocean anomalies during two prior months. These results reveal that the strong TWC anomalies during two prior months have an important role in the warm surface-layer temperature anomaly over the Siberia coastal regions.

For heavy snowfall February months, there are no significant differences in surface-layer ocean temperature in regions upstream of Iwamizawa (i.e., the northern Sea of Japan), even during prior months (December and January) (Fig. 6g-i). The no significant differences in warm surface-layer ocean anomalies indicate that the atmospheric circulation anomalies have important role in producing heavy snowfall over coastal regions of western Hokkaido during heavy snowfall February months. In addition, MTS has no significant correlation with surface-layer ocean temperature, even in the prior months (Fig. 7g–i). The surface-layer ocean temperature would have small impact on MTS during heavy snowfall February months.

The negative differences in turbulent heat flux between heavy and light snowfall years at Iwamizawa are seen over the northern Sea of Japan in all heavy snowfall months (Fig. 10), indicating that the anomalous upward latent heat flux over the northern Sea of Japan enhances snowfall over Sea of Japan side regions of Japan. To assess the impact of atmospheric and oceanic anomalies on turbulent heat flux anomaly, we further diagnosed the differences in contributions from SSTA, SATA and SWSA to turbulent heat flux anomaly (THFA) between heavy and light snowfall months for three winter months (Fig.11). In all heavy snowfall months, the contributions from SATA have almost the largest negative differences (<-40 W/m^{-2}) in with statistically significant over the entire northern Sea of Japan, meaning that SATA has the most important role in upward THFA (Fig. 11b,e and h). In the contributions from SWSA, negative differences (<–10 W/m^{-2}) are seen over the entire northern Sea of Japan in all heavy snowfall months (Fig. 11c,f and i). Although the magnitudes of negative differences in the contribution from SWSA are weaker than those from SATA, there are the relatively large negative differences (<–30 W/m^{-2}) over western Hokkaido coastal regions in heavy snowfall months December and February months (Fig. 11c and i). The SWSA over the entire northern Sea of Japan also contributes to upward THFA in all heavy snowfall months. In contrast, there are the differences in magnitude and distribution of SSTA contribution in each winter month (Fig, 11a,d and g). In heavy snowfall December months, the negative difference in SSTA over Ishikari Bay indicates that warm SST anomaly contributes to upward THFA over these regions (Fig, 11a). However, the amplitude of contribution from SSTA (>–10 W/m^{-2}) over Ishikari Bay are smaller than that from SATA and SWSA (Fig. 11a-c), meaning that the warm SST anomaly during heavy snowfall December months has minor impact on total snowfall at Iwamizawa compared with atmospheric contributions anomalies (temperature and wind speed). In heavy snowfall January months, the contribution from SSTA has relatively large negative value (<–30 W/m^{-2}) with the largest differences (<–50 W/m^{-2}) over the Siberia continent coastal regions (Fig. 11d). The relatively large contributions from SATA and SWSA are seen over the entire northern Sea of Japan (Fig. 11e and f). However, MTS at Iwamizawa has relatively strong positive correlations with turbulent heat flux over the Siberia continent coastal regions in January (not shown), meaning that upward turbulent heat flux over the Siberia continent coastal regions has the most important role in MTS at Iwamizawa in January. From these results, in heavy snowfall January months, the SSTA over the Siberia continent coastal region has an important role in heavy snowfall at Iwamizawa, as well as atmospheric contributions (i.e. SATA and SWSA). The maximum upward turbulent heat flux anomalies appear over regions downstream of the specific mountain lee side marking the initial point of formation of the thick cloud band (Muramatsu 1979; Ohtake et al. 2008). Over Siberia continent coastal regions, the warm surface-layer ocean anomaly would provide anomalous heat and moisture to atmosphere at initial formation of the cloud band.

3.3 Relationship between total snowfall at Iwamizawa and other Hokkaido regions

To investigate the distribution of MTS anomalies over Hokkaido when Iwamizawa experienced heavy snowfall events, we examined difference maps of MTS between heavy and light snowfall years for all winter months, produced using data from AMeDAS stations in Hokkaido (Fig. 12a–c). During all heavy snowfall winter months, the magnitudes of positive MTS in western Hokkaido are larger than those in eastern Hokkaido owing to the northwesterly winter monsoon over the Eurasian Continent. In heavy snowfall December months, the AMeDAS stations including Iwamizawa in coastal regions downstream of Ishikari Bay have relatively large positive MTS differences (i.e., >100 cm). Furthermore, the significant positive correlation of MTS amounts at AMeDAS stations in coastal regions of western Hokkaido near Ishikari Bay with MTS at Iwamizawa indicate that heavy snowfall at these stations coincide with heavy snowfall at Iwamizawa (Figs. 12d and 13a). In heavy snowfall January months, relatively large positive MTS differences are evident at AMeDAS stations near Iwamizawa (Fig. 12b). Moreover, the MTS at stations near Iwazamiwa has relatively high positive correlation with the MTS at Iwamizawa (Figs. 12e and 13b). The transports of airs over the Siberia continent coastal regions with the warm surface-layer ocean anomalies are seen near Iwamizawa (Figs. 6d, 10d), meaning that these surface-layer ocean anomalies influence snowfall at the AMeDAS stations near Iwazamiwa (Fig. 12b). In contrast, in heavy snowfall February months, AMeDAS stations with relatively large anomalies and high correlations are not limited to those near Iwamizawa (Figs. 12c,f and 13c). This is because heavy snowfall at Iwamizawa occurs even without the warm surface-layer ocean anomaly over the northern Sea of Japan when a cold outbreak associated with the northwesterly winter monsoon is strong.

4. Conclusions and discussion

Iwamizawa is in a region of western Hokkaido that experiences frequent heavy snowfall. This study used reanalysis data to investigate the atmospheric and oceanic circulation anomalies associated with heavy snowfall winter months at Iwamizawa. When heavy snowfall occurs at Iwamizawa, the anomalous northwesterly cold flow associated with a dipole pattern with an anticyclonic anomaly over the Eurasian Continent and a cyclonic anomaly over the northern Pacific Ocean causes cold temperatures over northern Japan during all winter months. In heavy snowfall December and January months, a preceding warm surface-layer ocean anomaly is evident in regions upstream of Iwamizawa during the one and two prior months. The MTS has statistically significant correlation with both the atmospheric circulations over East Asia and the surface-layer ocean temperatures in upstream regions in December and January. During these winter months, relatively large positive MTS anomalies are seen at several AMeDAS stations in coastal regions of western Hokkaido, particularly those near Iwamizawa. The analysis for evaluating the respective contribution from atmospheric (i.e. cold air temperature, strong wind speed anomalies) and oceanic (i.e. sea surface temperature anomaly) anomalies to turbulent heat flux anomaly indicate that the atmospheric contribution has the most important role in heavy snowfall in all heavy snowfall months. However, in heavy snowfall January months, the warm surface-layer ocean anomaly over the northern Sea of Japan associated with strong TWC anomaly also contributes to the increase in amount of snowfall at these stations.

The relationship between TWC volume transport at the Tsushima/Korea Strait during summer and autumn and precipitation on the Sea of Japan side of Japan in winter has been reported in previous studies (Hirose and Fukudome 2006, Hirose et al. 2009, Sugimoto and Hirose 2014). Hirose et al. (2009) found that the seasonal mean strength of the TWC at the Tsushima/Korea Strait during autumn (September–November) has positive correlation with both seasonal mean SST over the Sea of Japan and precipitation over Sea of Japan side regions during winter (December–February). Additionally, over the central Sea of Japan, the warm SST anomaly related to increase in TWC volume transport at the Tsushima/Korea Strait during the hot seasons (June–October) enhances the latent heat flux from the ocean, contributing to increased precipitation over northern Japan (Sugimoto and Hirose 2014). This investigation revealed that the strong TWC anomaly increases the surface-layer ocean temperature over the northern Sea of Japan, leading to an increase in the amount of snowfall at certain stations in coastal regions of western Hokkaido during January.

Linear positive trends of SST over the Sea of Japan from the late 1980s to the late 2010s are found during all winter months (Yasunaga and Tomochika 2017). Sensitivity experiments with different boundary conditions for SST over the Sea of Japan revealed that the latent heat flux increase associated with warm SST anomaly enhances the amount of precipitation over the Sea of Japan side of Japan (Takahashi et al. 2013). Thus, warm SST anomaly over the Sea of Japan would increase the amount of snowfall over western Hokkaido. Further investigation is required to better understand the potential future changes in precipitation over Hokkaido.

Acknowledgments

All JMA station datasets are available from the Japan Meteorological Agency (JMA) (https://www.jma.go.jp/jma/index.html). In this study, we used the Climate Forecast System Reanalysis data from January 1979 to March 2011 and Climate Forecast System Version 2 data after April 2011 (available from https://rda.ucar.edu/). The JMA radar and MSM data are available from the website of the Research Institute for Sustainable Humanosphere, Kyoto University (http://database.rish.kyoto-u.ac.jp/index-e.html). This work was supported by a Grant-in-Aid for Scientific Research (KAKENHI JP22K14103, JP19K14802, JP19K04647). We thank James Buxton MSc of Edanz (https://jp.edanz.com/ac) for correcting a draft of this manuscript. We would like to thank the editor, and the anonymous reviewers for their valuable comments regarding improvement of the manuscript.

References

Ando, Y., M. Ogi and Y. Tachibana, 2015: Abnormal Winter Weather in Japan during 2012 Controlled by Large-Scale Atmospheric and Small-Scale Oceanic Phenomena, *Mon. Wea. Rev.*, 143, 54–63, https://doi.org/10.1175/MWR-D-14-00032.1

Campbell, S. L., J. W. Steenburgh, Y. Yamada, M, Kawashima and Y. Fujiyoshi, 2018: Influences of orography and coastal geometry on a transverse-mode sea-effect snowstorm over Hokkaido Island, Japan. *Mon. Wea. Rev.*, 146(7), 2201–2220. https://doi.org/10.1175/MWR-D-17-0286.1

Fujiyoshi, Y., K. Tsuboki, S. Satoh, and G. Wakahama, 1992: Three dimensional radar echo structure of a snow band formed on the lee side of a mountain. *J. Meteor. Soc. Japan*, 70, 11–24.

Fujiyoshi, Y., N. Yoshimoto, and T. Takeda, 1998: A dual-Doppler radar study of longitudinal-mode snowbands. Part I: A three-dimensional kinematic structure of meso-g-scale convective cloud systems within a longitudinal-mode snowband. *Mon. Wea. Rev.*, 126, 72–91.

Hirose, N. and K. Fukudome, 2006: Monitoring the Tsushima warm current improves seasonal prediction of the regional snowfall. *SOLA*, 2, 61–63.

Hirose,N., K. Nishimura, and M. Yamamoto, 2009: Observational evidence of a warm ocean current preceding a winter teleconnection pattern in the northwestern Pacific, *Geophys. Res. Lett.*, 36, L09705, doi:10.1029/2009GL037448.

Honda M, J. Inoue, and S. Yamane, 2009: Influenec of low Arctic seaice minima on anomalously cold Eurasian winters, *Geophys. Res. Lett.*, 36, L08707.

Hori, E. M., J. Inoue, T. Kikuchi, M. Honda, and Y. Tachibana, 2011: Recurrence of Intraseasonal Cold Air Outbreak during the 2009/2010 Winter in Japan and its Ties to the Atmospheric Condition over the Barents-Kara Sea. *SOLA*, 2, 61–63.

Inatsu, M., S. Tanji, and Y. Sato, 2020: Toward predicting expressway closures due to blowing snow events. *Cold Region Science and Technology*, 177, 103-123.

Inatsu, M., S. Kawazoe, and M. Mori, 2021: Trends and projection of heavy snowfall in Hokkaido, Japan as an application of self-organizing map. *Journal of Applied Meteorology and Climatology*, doi:10.1175/JAMC-D-21-0085.1

Inoue, J., M. Kawashima, Y. Fujiyoshi, and M. Yoshizaki, 2005: Aircraft observations of air-mass modification upstream of the Sea of Japan during cold-air outbreaks. *J. Meteorol. Soc. Japan*, 83, 189–200.

Inoue, J., M. E. Hori, and K. Takaya, 2012: The role of Barents Sea ice in the wintertime cyclone track and emergence of a warm-Arctic cold-Siberian anomaly. *J. Clim.,* 25, 2561–8.

Katsumata, M., H. Uyeda, and K. Kikuchi, 1998: Characteristics of a cloud band off. the west coast of Hokkaido Island as determined from AVHRR/NOAA, SSM/I and radar data. *J. Meteor. Soc. Japan*, 76, 169–189.

Katsumata, M., H. Uyeda, K. Iwanami, and G. Liu, 2000: The response of 36- and 89-GHz microwave channels to convective snow clouds over ocean: Observation and modeling. *J. Appl. Meteor.*, 39, 2322–2335.

Kawazoe, S., M. Inatsu, T. J. Yamada, and T. Hoshino, 2020: Climate change impacts on heavy snowfall in Sapporo using 5-km mesh large ensemble simulations. *SOLA*, 16, 233−239, doi:10.2151/sola.2020-039.

Kunoki, S., and Coauthors, 2015: Oceanic influence on the Baiu frontal zone in the East China Sea. *J. Geophys. Res. Atmos.*, 120, 449–463, doi:10.1002/2014JD022234.

Manda, A. et al., (2014): Impacts of a warming marginal sea on torrential rainfall organized under the Asian summer monsoon. *Sci. Rep.*, 4, 5741, doi:10.1038/srep05741.

Minobe, S., A. Kuwano-Yoshida, N. Komori, S.-P. Xie, R. J. Small, 2008: Influence of the Gulf Stream on the troposphere. *Nature*, 452(7184). U206–U251. doi:10.1038/nature06690

Minobe, S., M., Miyashita, A. Kuwano-Yoshida, H. Tokinaga, S.-P. Xie, 2010: Atmospheric response to the Gulf Stream: seasonal variations. *J. Clim*., 23(13), 3699–3719. doi:10.1175/2010jcli3359.1

Minobe S. and S. Takebayashi, 2015: Diurnal precipitation and high cloud frequency variability over the Gulf Stream and over the Kuroshio, *Clim. Dyn.*, 44, 2079–2095, DOI 10.1007/s00382-014-2245-y

Mori, M., M. Watanabe, H. Shiogama, J. Inoue, and M. Kimoto, 2014: Robust Arctic sea-ice influence on the frequent Eurasian cold winters in past decades. *Nat. Geosci.*, 7, 869–73.

Muramatsu, T., 1979: The cloud line enhanced by upwind orographic features in winter monsoon situations. *Geophys. Mag.*, 38, 1–15.

Nakamura, T., K. Yamazaki, K. Iwamoto, M. Honda, Y. Miyoshi, Y. Ogawa, and J. Ukita, 2015: A negative phase shift of the winter AO/NAO due to the recent Arctic sea-ice reduction in late autumn, *J. Geophys. Res. Atmos.*, 120, 3209–3227, doi:10.1002/2014JD022848.

Nakanowatari, T., K. Sato, and J. Inoue, 2014: Predictability of the Barents Sea ice in early winter: remote effects of oceanic and atmospheric thermal conditions from the North Atlantic. *J. Clim.*, 27, 8884–901.

Ninomiya, K., 1968: Heat and water budget over the Japan Sea and the Japan Islands in winter season. *J. Meteorol. Soc. Japan,* 46 (5), 343-372.

Ninomiya, K., 1994: Meso-scale low family formed over the northeastern Japan Sea in the northwestern part of a parent polar low. *J. Meteor. Soc. Japan*, **72**, 589–603, https://doi.org/10.2151/jmsj1965.72.4_589.

Ohtake, H., M. Kawasaki, and Y. Fujiyoshi, 2008: The Formation Mechanism of a Thick Cloud Band over the Northern Part of the Sea of Japan during Cold Air Outbreaks. *J. Meteorol. Soc. Japan,* 87, 289-306.

Saha, S. *et al.* 2010: The NCEP climate forecast system reanalysis. *Bull. Am. Meteorol. Soc.,* **91(8).** 1015–1057. doi:10.1175/2010BAMS3001.1

Saha, S. *et al.* 2014: The NCEP climate forecast system version 2. *J. Clim,* **27,** 2185–208.

Sato, T. and S. Sugimoto, 2013: A numerical experiment on the influence of the interannual variation of sea surface temperature on terrestriall precipitateon in northern Japan during the cold season. *Water Resources Research*, 49, 7763-7777.

Sato, K, J. Inoue, and M. Watanabe, 2014: Influence of the Gulf Stream on the Barents Sea ice retreat and Eurasian coldness during early winter. *Environ. Res. Lett.*, **9**, 084009.

Sato, K. et al., 2015: Influence of the Kuroshio on mesoscale convective systems in the baiu frontal zone over the East China Sea, *Mon. Wea. Rev.*, 144(3), 1017-1033.

Sato, K., J. Inoue, A. Yamazaki, J.-H. Kim, M. Maturilli, K. Dethloff, S. R. Hudson, and M. A. Granskog, 2017: Improved forecasts of winter weather extremes over midlatitudes with extra Arctic observations, *J. Geophys. Res. Oceans*, 121, doi:10.1002/2016JC012197.

Sato K, J. Inoue, I. Simmonds, and I. Rudeva, 2021: Antarctic Peninsula warm winters influenced by Tasman Sea temperatures. *Nature Comms.*, **12,** 1497, doi: 10.1038/s41467-021-21773-5.

Shirakawa, T. and T. Kameda, 2019: Snow surveys of central and eastern Hokkaido from 2014 to 2018, and meteorological elements affecting snow grain type, *Seppyo*, 81(4), 163-182 (in Japanese).

Sugimoto, S. and N. Hirose, 2014: Variations in latent heat flux over the eastern Japan Sea in December. *SOLA*, 10, 1−4, doi:10.2151/sola.2014-001.

Takahashi, H. G. and T. Idenaga, 2013: Impact of SST on precipitation and snowfall on the sea of Japan side in the winter monsoon season: timescale dependency. *J. Meteor. Soc. Japan*, 91(5), 639–653.

Takahashi, H. G., N. N. Ishizaki, H. Kawase, M. Hara, T. Yoshikane, X. Ma and F. Kimura, 2013: Potential impact of sea surface temperature on winter precipitation over the Japan Sea side of Japan: a regional climate modeling study. *J. Meteor. Soc. Japan*, 91(4), 471–488.

Takahashi, H. G. 2021: Longterm trends in snowfall characteristics and extremes in Japan from 1961 to 2012. *Int. J. Climatol.*, 41, 2316– 2329. https://doi.org/10.1002/joc.6960.

Takano, Y., Y. Tachibana, and K. Iwamoto, 2008: Influences of Large-scale Atmospheric Circulation and Local Sea Surface Temperature on Convective Activity over the Sea of Japan in December. *SOLA*, 4, 113–116.

Takaya, K. and H. Nakamura, 2013: Interannual variability of the East Asian winter monsoon and related modulations of the Planetary wave. *J. Clim.*, 26, 9445–9461.

Tanimoto, Y., H. Nakamura, T. Kagimoto, and S. Yamane, 2003: An active role of extratropical sea surface temperature anomalies in determining anomalous turbulent heat flux, *J. Geophys. Res.*, 108(C10), 3304, doi:10.1029/2002JC001750.

Tsuboki, K., Y. Fujiyoshi, and G. Wakahama, 1989: Doppler radar observation of convergence band cloud formed on the west coast of Hokkaido island. II: Cold frontal type. J. Meteor. Soc. Japan, 67, 985– 999.

Yasunaga, K. and M. Tomochika, 2017: An increasing trend in the early winter precipitation during recent decades along the coastal areas of the sea of Japan. *Journal of Hydrometeorology*, 18(11), 2893–2906.

Yoshimoto, N., Y. Fujiyoshi, and T. Takeda, 2000: A dual-Doppler radar study of longitudinal-mode snowbands. Part II: Influence of the kinematics of a longitudinal-mode snowband on the development of an adjacent snowband. *J. Meteor. Soc. Japan*, 78, 381–403.

Yoshizaki, M., T. Kato, H. Eito, S. Hayashi, and W. Tao, 2004: An overview of the field experiment ''Winter mesoscale convective systems (MCSs) over the Japan sea in 2001'', and comparisons of the cold-air outbreak case (14 January) between analysis and a non-hydrostatic cloud-resolving model. *J. Meteor. Soc. Japan*, 82, 1365–1387.

List of Figures:

Figure 1. Climatological total snowfall (MTS) at 116 Automated Meteorological Data Acquisition System (AMeDAS) stations in Hokkaido during three winter months (December-February) from 1979/1980 to 2020/2021. Red square shows location of Iwamizawa station.

Figure 2. (a) Time series of snow depth (red line: cm) and daily snowfall (black bars: cm) at Iwamizawa station. Precipitation intensity measured by Japan Meteorological Agency (JMA) radars (shading: mm/hr) and geopotential height (contours: m) with wind velocity (vector: m/s) at 850-hPa level based on JMA Meso Scale Model data (MSM) at (b) 09:00 UTC December 1, 2020, (c) 15:00 UTC December 13, 2020, (d) 00:00 UTC February 9, 2021, and (e) 00:00 UTC February 24, 2021. Colored dots show accumulated snowfall at AMeDAS stations during each snowfall event (SE 1: 01-02 December 2020, SE2: 13-14 December 2020, SE 3: 08-09 February 2021, SE 4: 23-24 February 2021).

Figure 3. Time series of monthly total snowfall (MTS) anomalies (deviation from climatology for 1979–2021) at Iwamizawa station during 1979 and 2021 (2020 for December): (a) December, (b) January, and (c) February. Red (blue) dots indicate years with heavy (light) snowfall considered in the study. Dashed lines show the 0.7 standard deviation.

Figure 4. Difference maps of air temperature at 950 hPa (T950) (°C: shading) with sea level pressure (hPa: contours) between heavy and light monthly total snowfall at Iwamizawa: (a) December, (b) January, and (c) February. Dot areas denote significant differences exceeding the 90% confidence level. (d)–(f) Same as (a)–(c) but for sea ice concentration (%: shading) with geopotential height (m: contours) and wave activity fluxes at 300 hPa (WAF300) (m/s^2: vectors).

Figure 5. Correlation coefficients of monthly total snowfall (MTS) at Iwamizawa with air temperature at 950 hPa (T950): (a) December, (b) January, and (c) February. Cross-hatched areas denote significant differences exceeding the 90% confidence level. (d)–(f) Same as (a)–(c) but for MTS with geopotential height at 300 hPa (Z300).

Figure 6. Difference maps of ocean temperature (°C: shading) with ocean currents (m/s: vectors) at 5-m depth between heavy and light snowfall Decembers at Iwamizawa for (a) 0 month (December), (b) -1 month (November), and (c) -2 month (October) lag times. Gray shading represents data that were not significant at the 90% confidence level. Black dot shows location of Iwamizawa station. (d)–(f) and (g)–(i) Same as (a)–(c) but for January and February, respectively.

Figure 7. Correlation coefficients of monthly total snowfall (MTS) at Iwamizawa during December with ocean temperature in the surface layer (5-m depth) for (a) 0 month (December), (b) -1 month (November), and (c) -2 month (October) lag times. Gray shading represents data that were not significant at the 90% confidence level. (d)–(f) and (g)–(i) Same as (a)–(c) but for January and February, respectively.

Figure 8. Same as Fig. 6 but for contribution from horizontal temperature advection to heat balance in the surface-layer ocean.

Figure 9. Same as Fig. 6 but for surface heat flux (W/ m^2: shading). Negative value shows upward direction from ocean to atmosphere.

Figure 10. Difference maps of surface heat flux (W/m^2: shading) and wind velocity at 10m (m/s: vector) between heavy and light snowfall at Iwamizawa for (a) Decembers, (b) Januarys and (c) Februarys, respectively. Gray shading represents data that were not significant at the 90% confidence level. Black dot shows location of Iwamizawa station. Negative value shows upward direction from ocean to atmosphere.

Figure 11. Difference maps of contributions from (a) sea surface temperature anomaly (SSTA: W/ m^2), (b) surface air temperature anomaly (SATA: W/ m^2) and (c) surface wind speed anomaly (SWSA: W/ m^2) between heavy and light snowfall Decembers at Iwamizawa. Negative value shows upward direction from ocean to atmosphere. Cross-hatched areas denote significant differences exceeding the 90% confidence level. (d)–(f) and (g)–(i) Same as (a)–(c) but for January and February, respectively.

Figure 12. (a) Difference maps of monthly total snowfall (MTS) at AMeDAS stations in Hokkaido between heavy and light snowfall months at Iwamizawa: (a)

December, (b) January, and (c) February. Red square shows location of Iwamizawa station. (d)–(f) Same as (a)–(c) but for correlation coefficients of monthly total snowfall (MTS) between Iwamizawa and each AMeDAS station.

Figure 13. Scatter plots of correlation coefficients of monthly total snowfall (MTS) and distances between Iwamizawa and each AMeDAS station for (a) December, (b) January and (c) February.

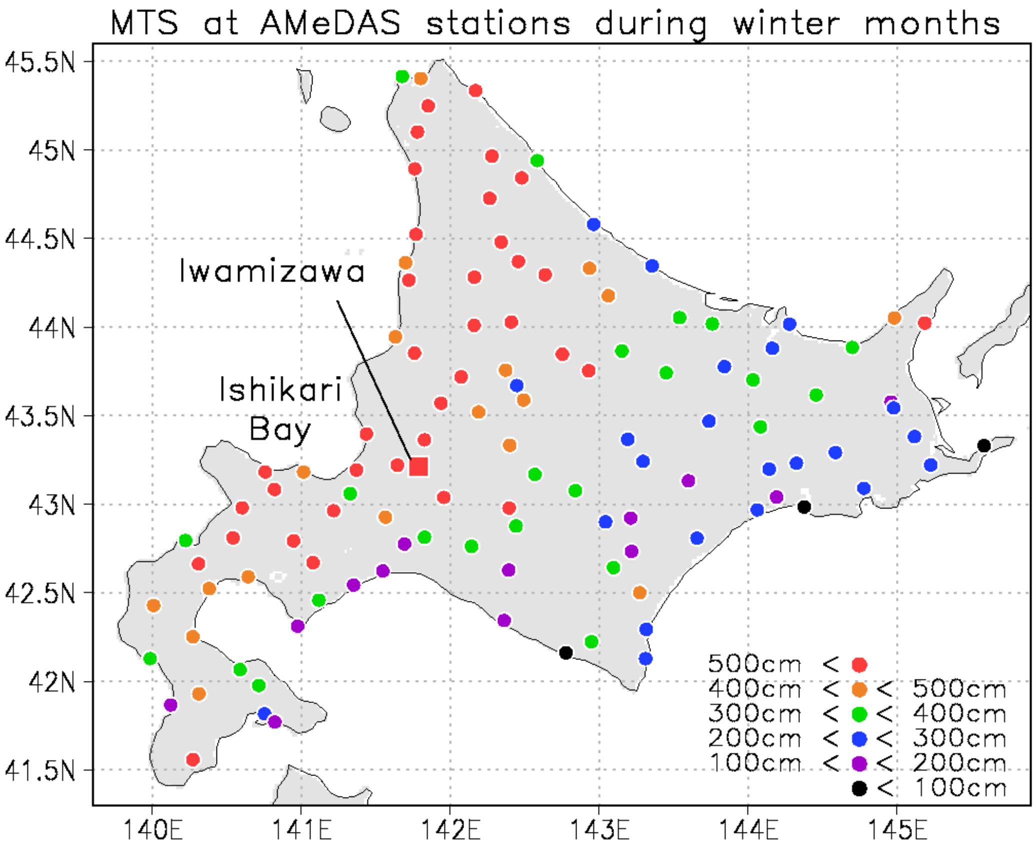

Figure 1. Climatological total snowfall (MTS) at 116 Automated Meteorological Data Acquisition System (AMeDAS) stations in Hokkaido during three winter months (December-February) from 1979/1980 to 2020/2021. Red square shows location of Iwamizawa station.

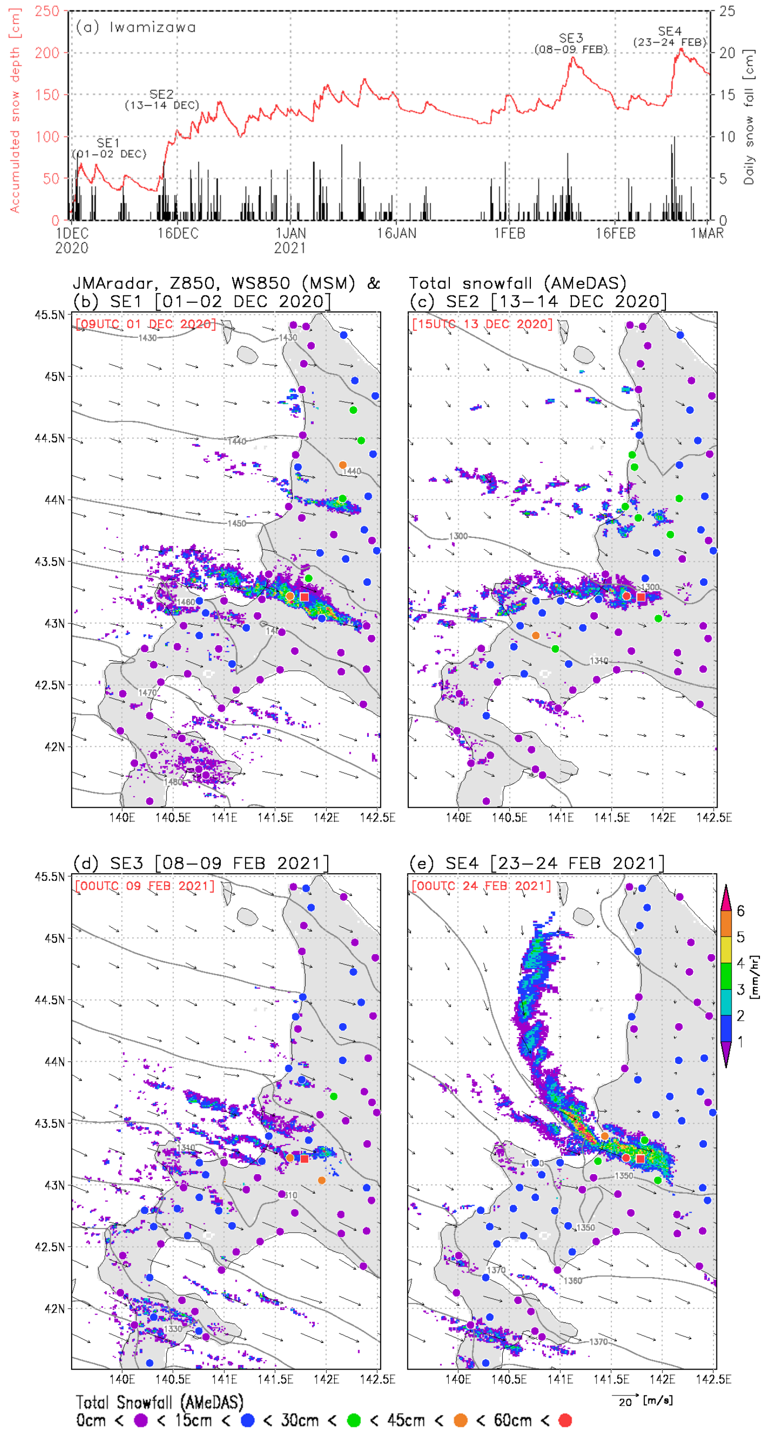

Figure 2. (a) Time series of snow depth (red line: cm) and daily snowfall (black bars: cm) at Iwamizawa station. Precipitation intensity measured by Japan Meteorological Agency (JMA) radars (shading: mm/hr) and geopotential height (contours: m) with wind velocity (vector: m/s) at 850-hPa level based on JMA Meso Scale Model data (MSM) at (b) 09:00 UTC December 1, 2020, (c) 15:00 UTC December 13, 2020, (d) 00:00 UTC February 9, 2021, and (e) 00:00 UTC February 24, 2021. Colored dots show accumulated snowfall at AMeDAS stations during each snowfall event (SE 1: 01-02 December 2020, SE2: 13-14 December 2020, SE 3: 08-09 February 2021, SE 4: 23-24 February 2021).

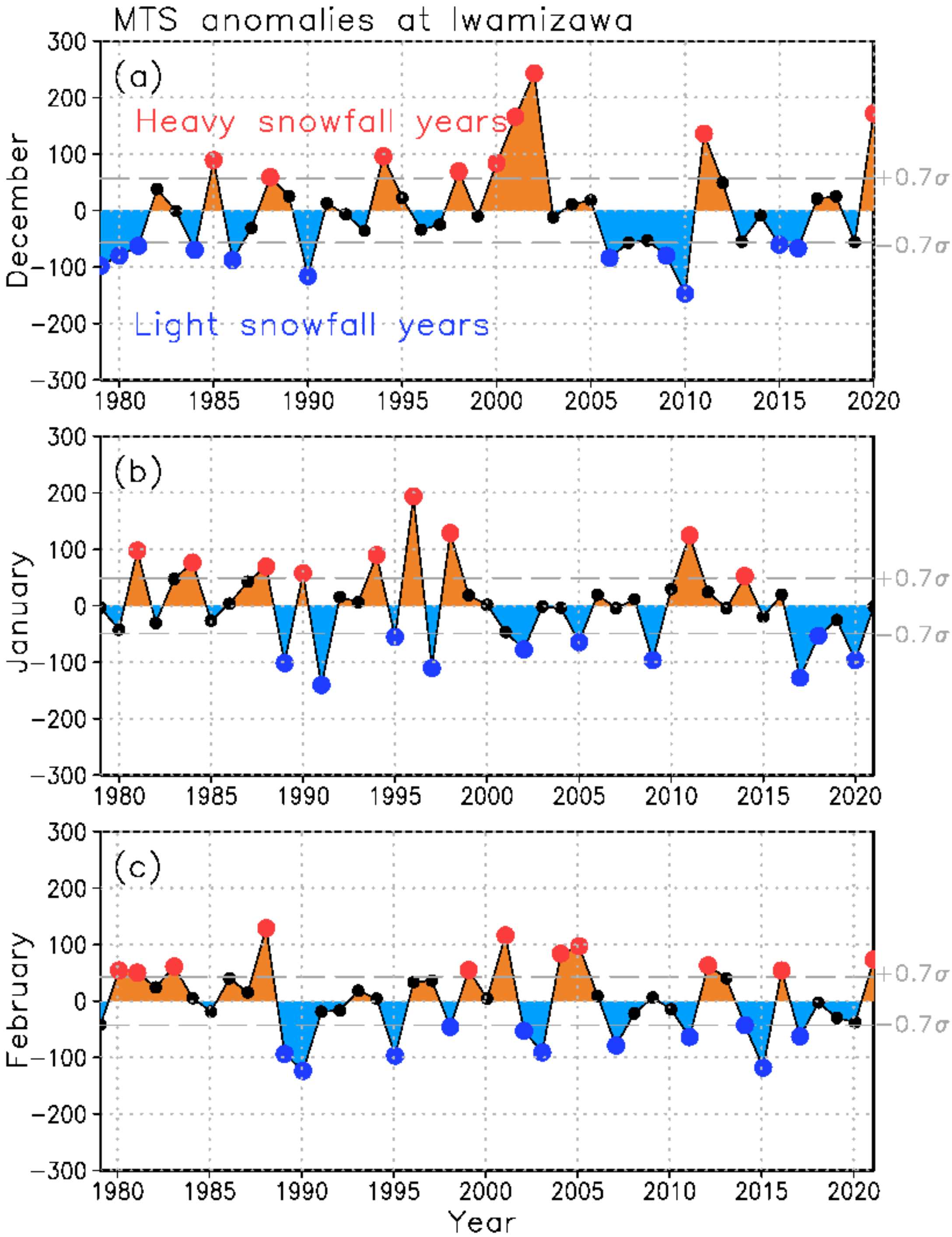

Figure 3. Time series of monthly total snowfall (MTS) anomalies (deviation from climatology for 1979–2021) at Iwamizawa station during 1979 and 2021 (2020 for December): (a) December, (b) January, and (c) February. Red (blue) dots indicate years with heavy (light) snowfall considered in the study. Dashed lines show the 0.7 standard deviation.

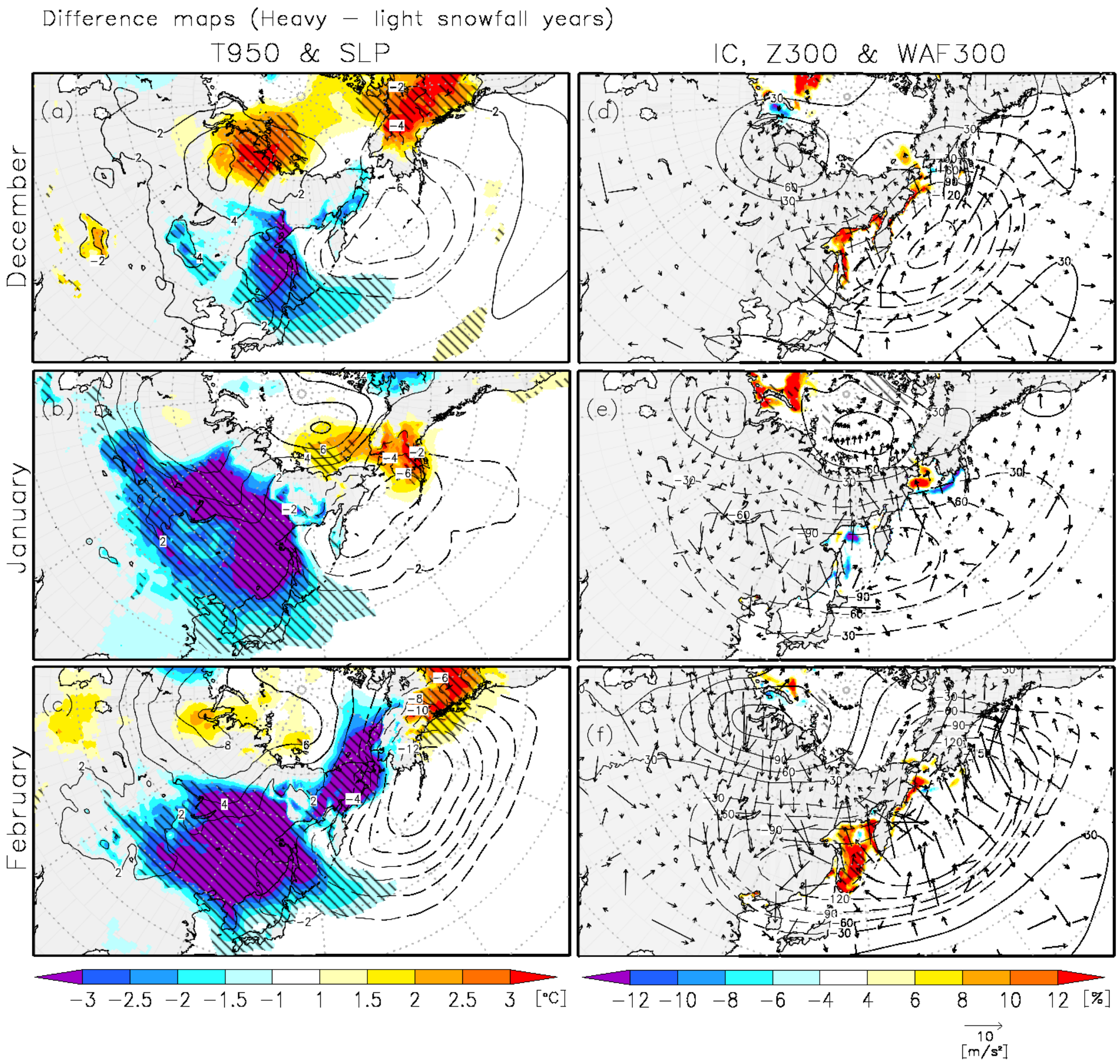

Figure 4. Difference maps of air temperature at 950 hPa (T950) (°C: shading) with sea level pressure (hPa: contours) between heavy and light monthly total snowfall at Iwamizawa: (a) December, (b) January, and (c) February. Cross-hatched areas denote significant differences exceeding the 90% confidence level. (d)–(f) Same as (a)–(c) but for sea ice concentration (%: shading) with geopotential height (m: contours) and wave activity fluxes at 300 hPa (WAF300) (m/s^2: vectors).

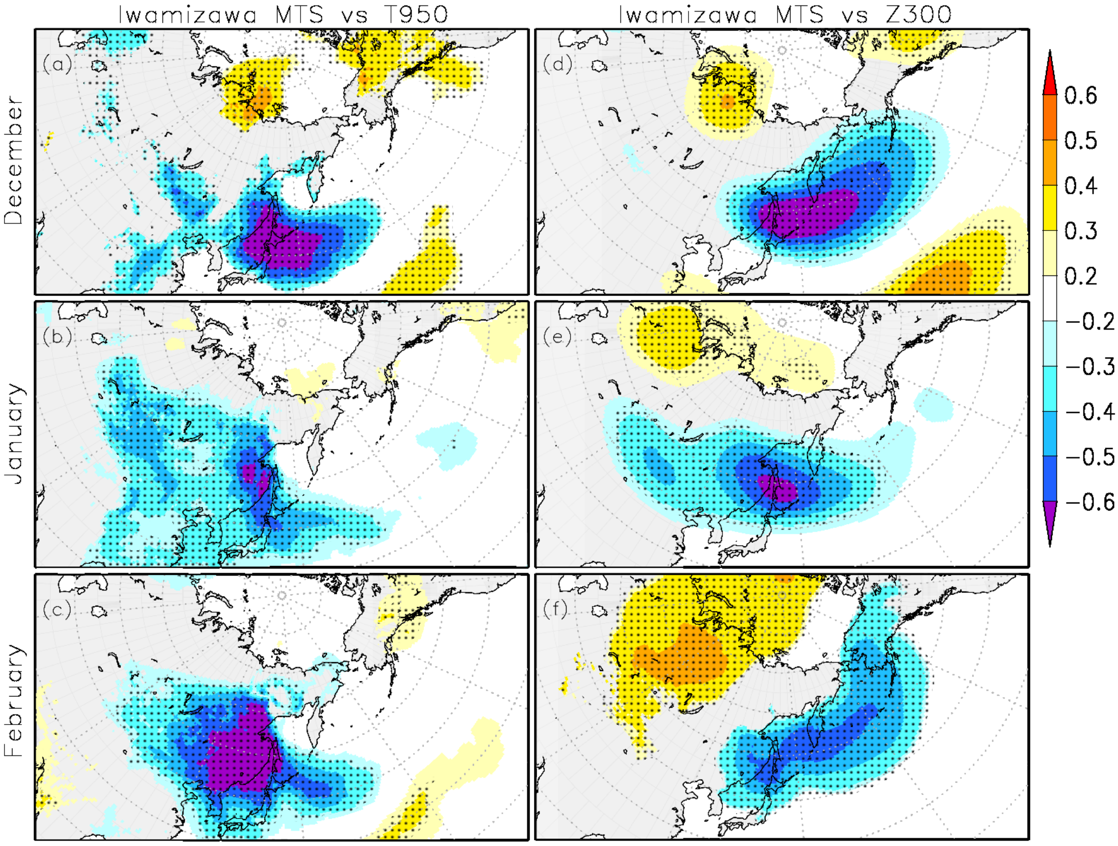

Figure 5. Correlation coefficients of monthly total snowfall (MTS) at Iwamizawa with air temperature at 950 hPa (T950): (a) December, (b) January, and (c) February. Dot areas denote significant differences exceeding the 90% confidence level. (d)–(f) Same as (a)–(c) but for MTS with geopotential height at 300 hPa (Z300).

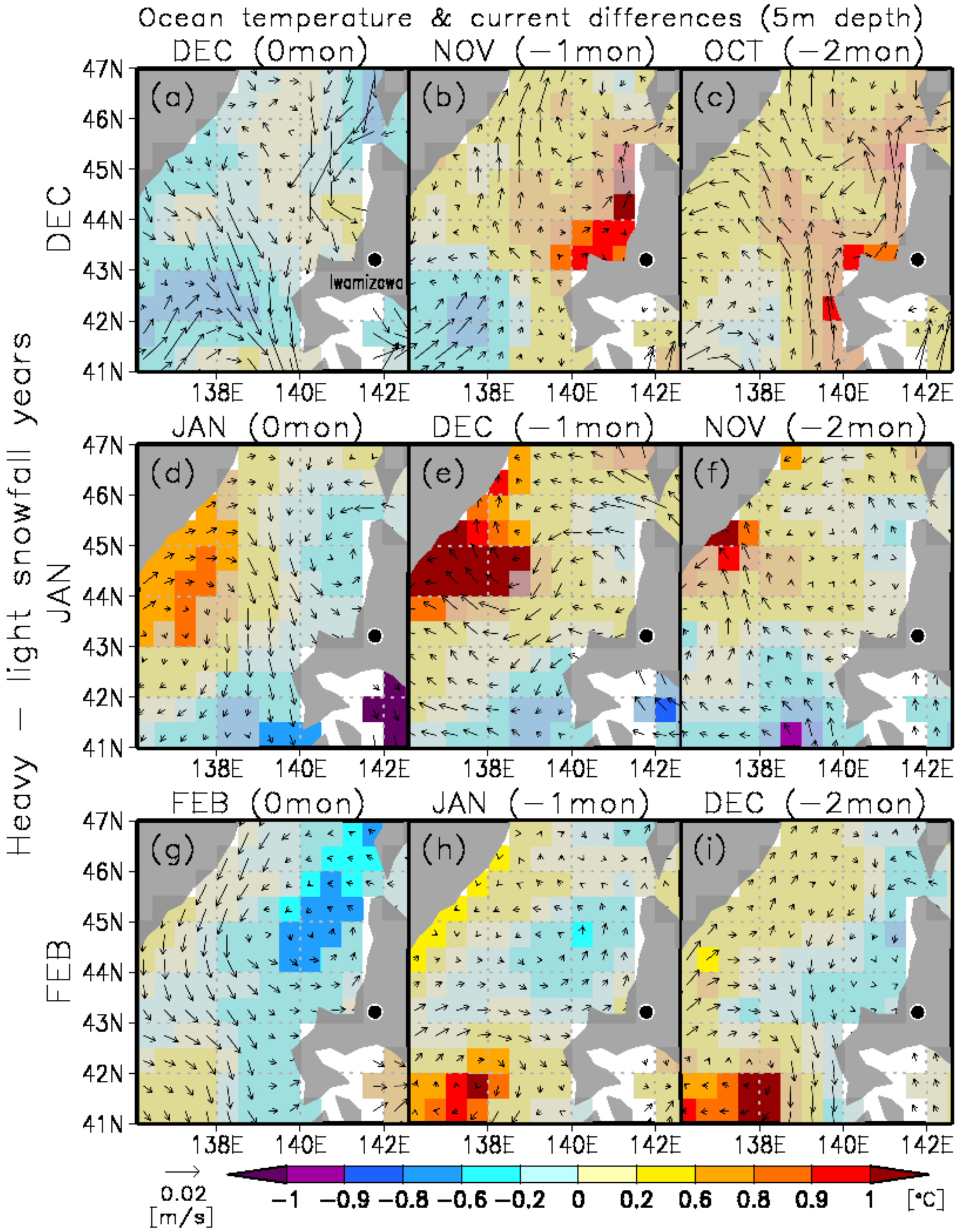

Figure 6. Difference maps of ocean temperature (°C: shading) with ocean currents (m/s: vectors) at 5-m depth between heavy and light snowfall Decembers at Iwamizawa for (a) 0 month (December), (b) -1 month (November), and (c) -2 month (October) lag times. Gray shading represents data that were not significant at the 90% confidence level. Black dot shows location of Iwamizawa station. (d)–(f) and (g)–(i) Same as (a)–(c) but for January and February, respectively.

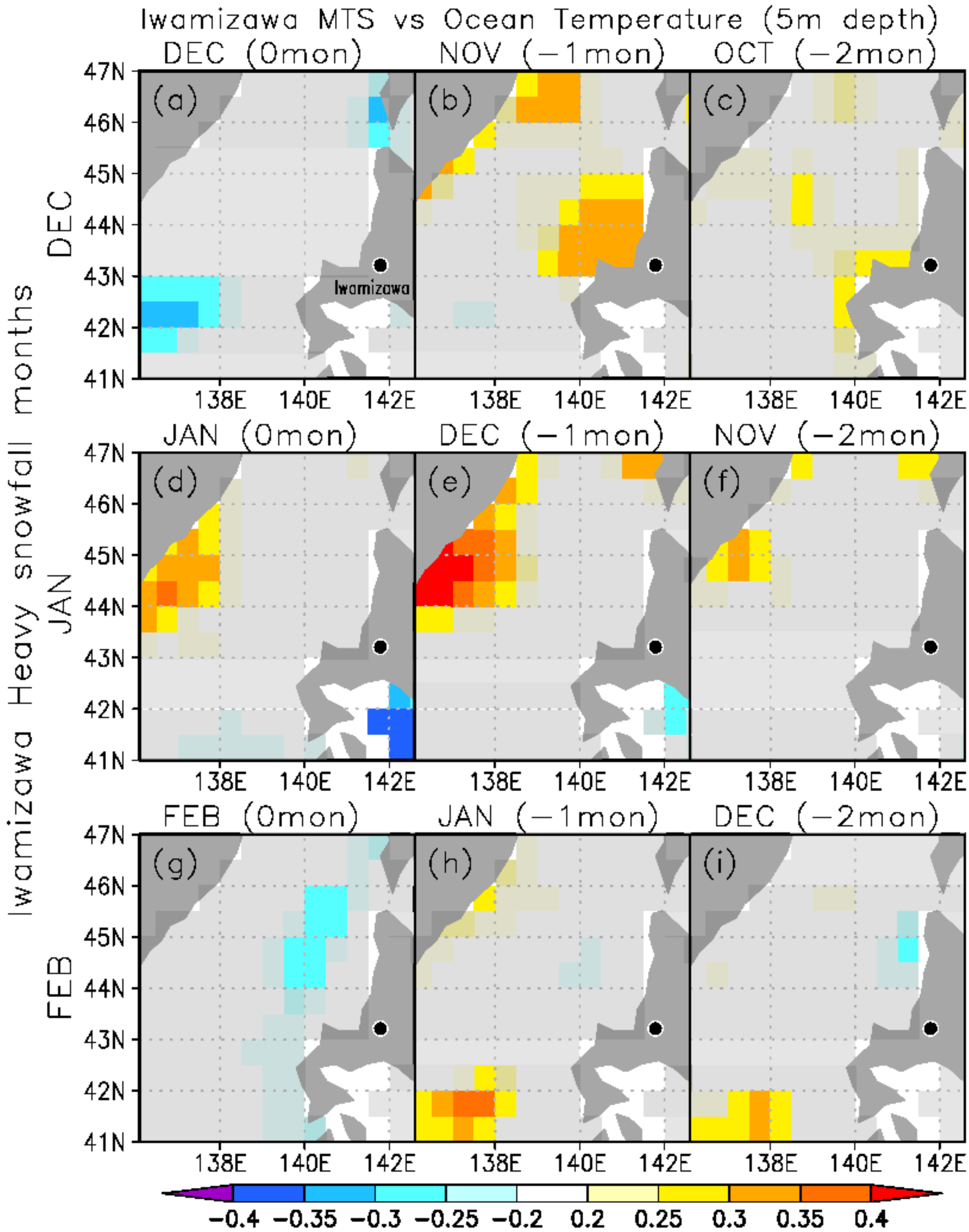

Figure 7. Correlation coefficients of monthly total snowfall (MTS) at Iwamizawa during December with ocean temperature in the surface layer (5-m depth) for (a) 0 month (December), (b) -1 month (November), and (c) -2 month (October) lag times. Gray shading represents data that were not significant at the 90% confidence level. (d)–(f) and (g)–(i) Same as (a)–(c) but for January and February, respectively.

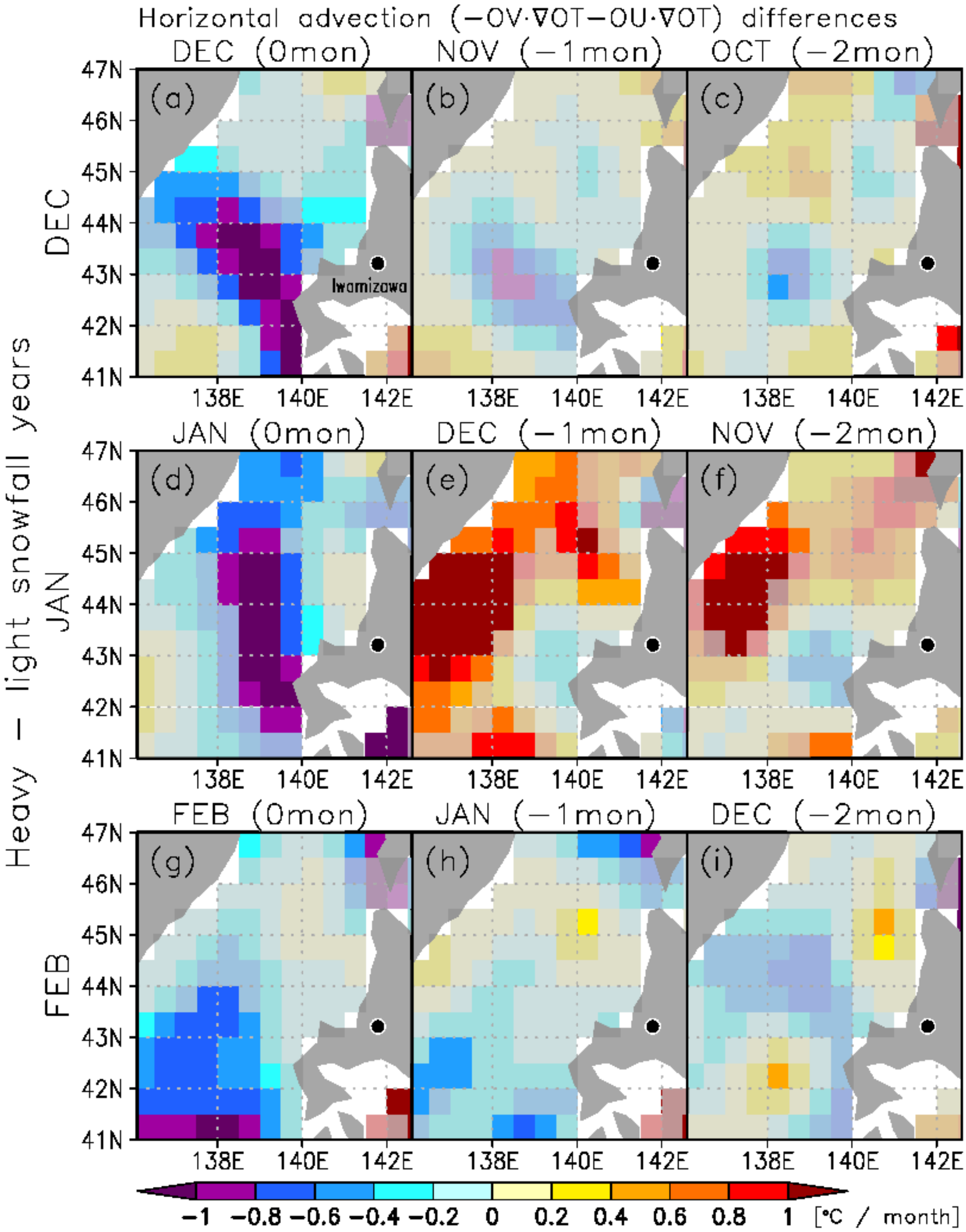

Figure 8. Same as Fig. 6 but for contribution from horizontal temperature advection to heat balance in the surface-layer ocean.

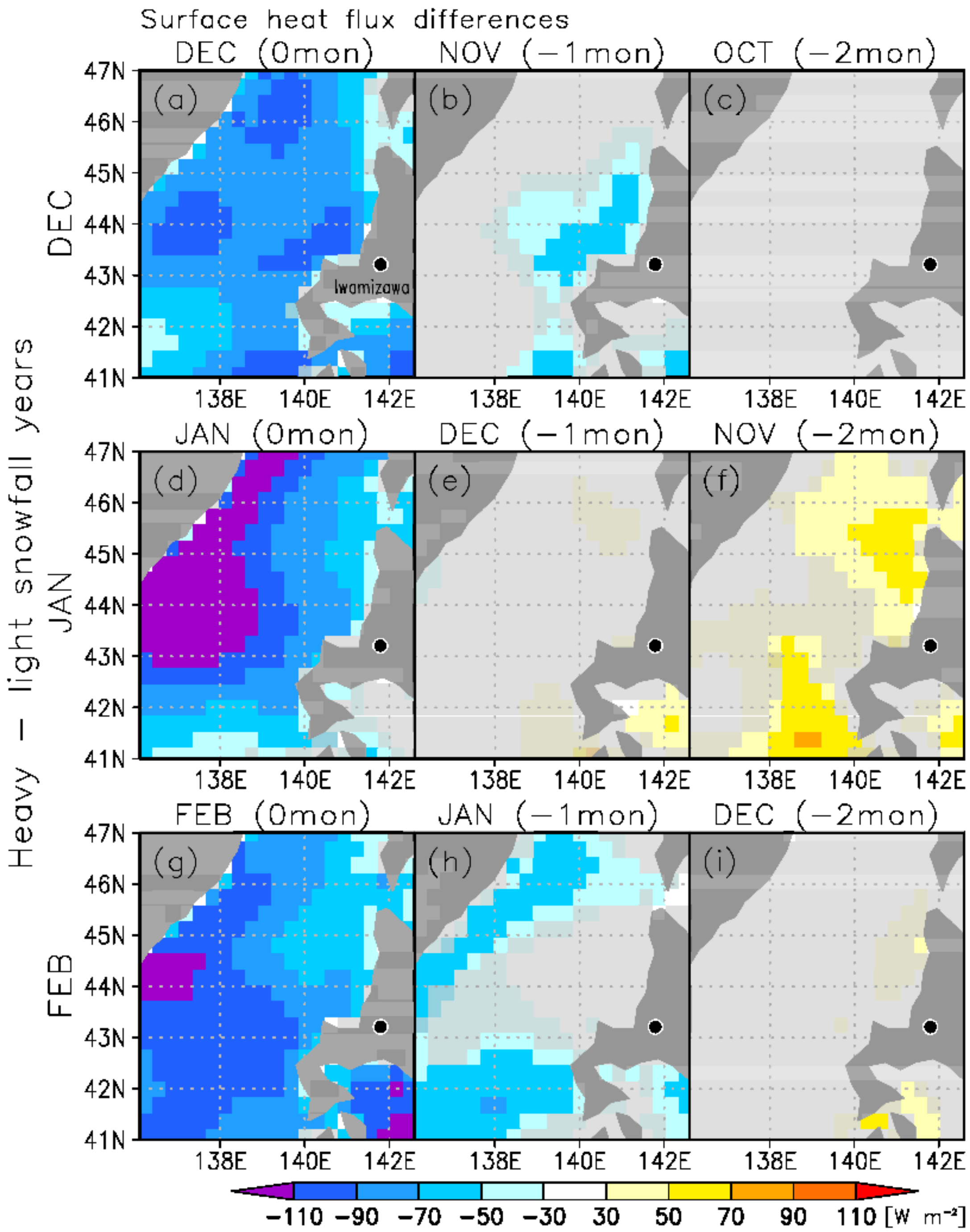

673 Figure 9. Same as Fig. 6 but for surface heat flux (W/ m^2: shading). Negative value shows upward
674 direction from ocean to atmosphere.

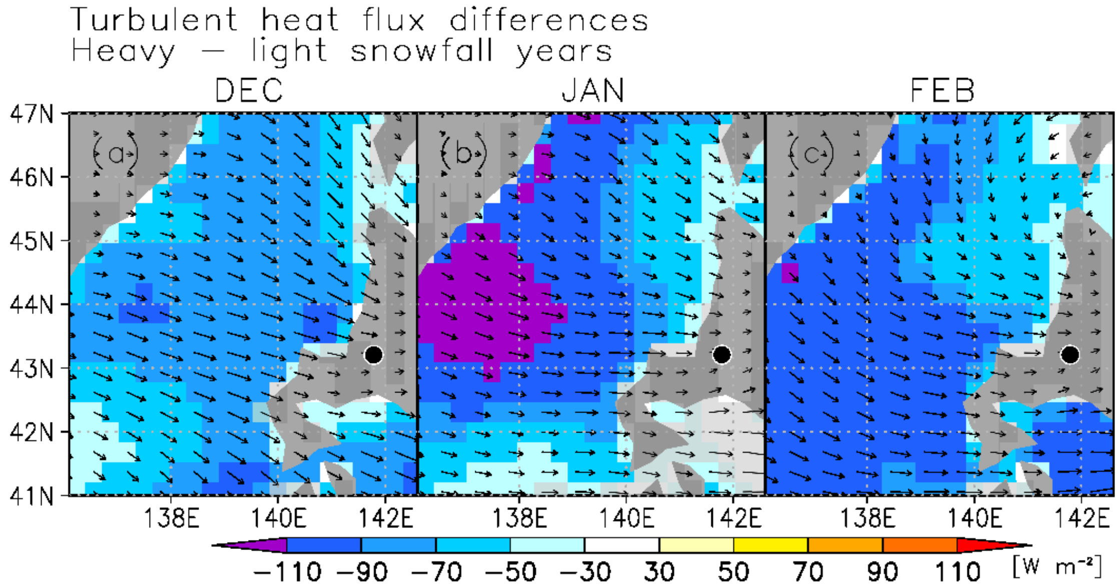

Figure 10. Difference maps of surface heat flux (W/m^2: shading) and wind velocity at 10m (m/s: vector) between heavy and light snowfall at Iwamizawa for (a) Decembers, (b) Januarys and (c) Februarys, respectively. Gray shading represents data that were not significant at the 90% confidence level. Black dot shows location of Iwamizawa station. Negative value shows upward direction from ocean to atmosphere.

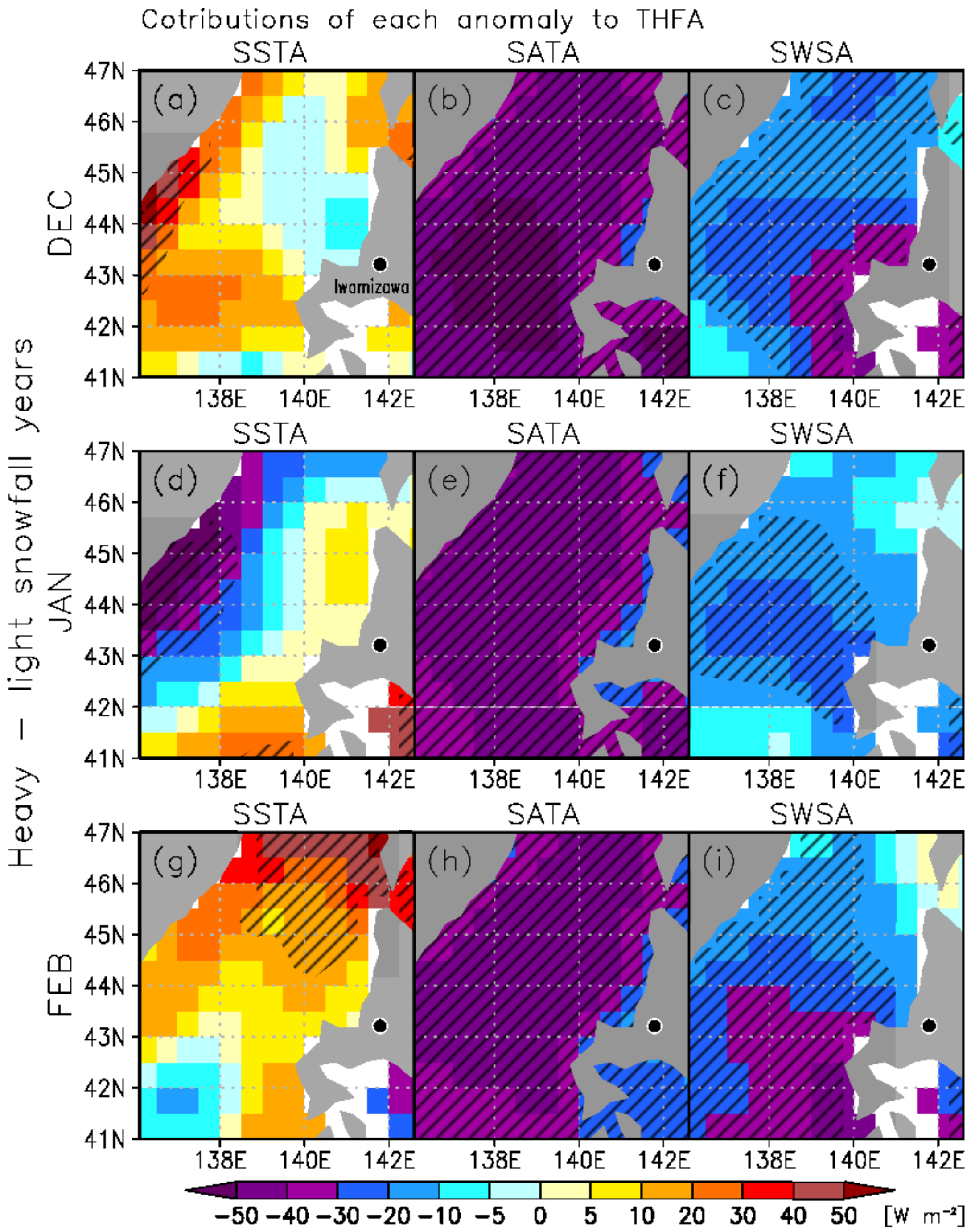

Figure 11. Difference maps of contributions from (a) sea surface temperature anomaly (SSTA: W/ m^2), (b) surface air temperature anomaly (SATA: W/ m^2) and (c) surface wind speed anomaly (SWSA: W/ m^2) between heavy and light snowfall Decembers at Iwamizawa. Negative value shows upward direction from ocean to atmosphere. Cross-hatched areas denote significant differences exceeding the 90% confidence level. (d)–(f) and (g)–(i) Same as (a)–(c) but for January and February, respectively.

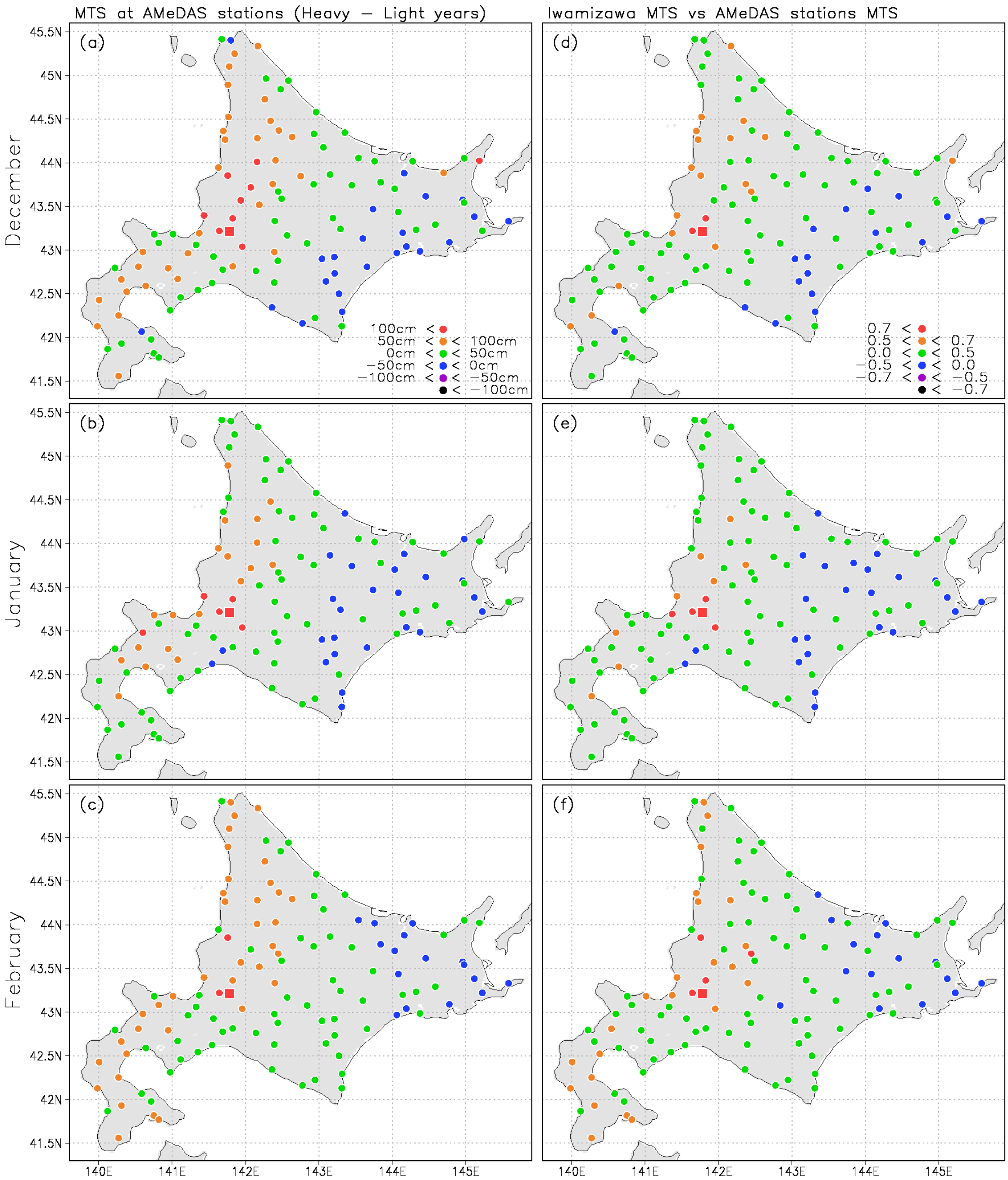

Figure 12. (a) Difference maps of monthly total snowfall (MTS) at AMeDAS stations in Hokkaido between heavy and light snowfall months at Iwamizawa: (a) December, (b) January, and (c) February. Red square shows location of Iwamizawa station. (d)–(f) Same as (a)–(c) but for correlation coefficients of monthly total snowfall (MTS) between Iwamizawa and each AMeDAS station.

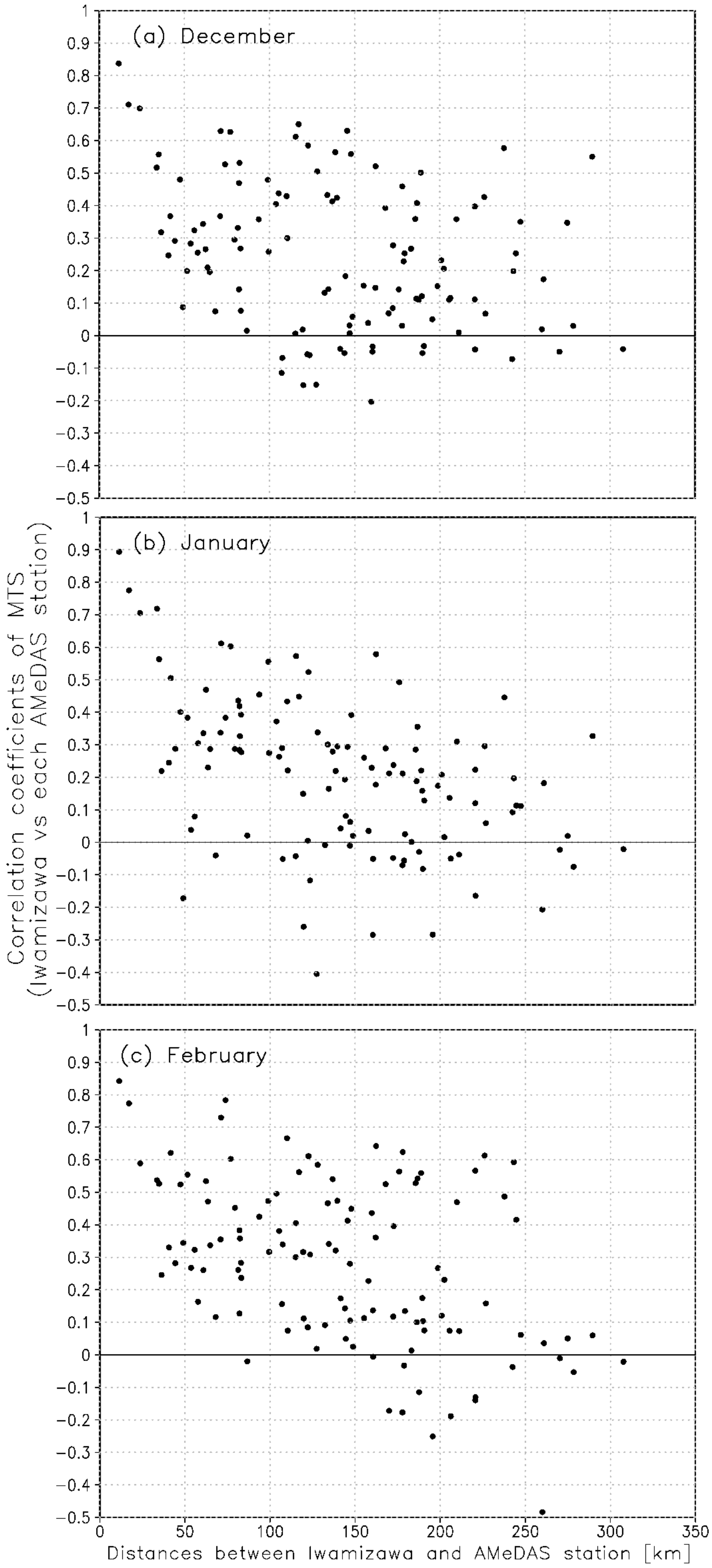

/41

Figure 13. Scatter plots of correlation coefficients of monthly total snowfall (MTS) and distances between Iwamizawa and each AMeDAS station for (a) December, (b) January and (c) February.